

Vibrational properties of Al_2O_3 films on gold, aluminum, and silicon

P. Brüesch, R. Kötz, H. Neff, and L. Pietronero

Brown Boveri Research Center, CH-5405 Baden, Switzerland

(Received 18 July 1983)

The vibrational properties of thin films of Al_2O_3 on Au, Al, and Si have been studied by means of infrared reflection absorption spectroscopy (IRAS). The films have been characterized by x-ray photoelectron spectroscopy (XPS), ultraviolet photoelectron spectroscopy (UPS), transmission electron microscopy, and low-angle x-ray experiments. The latter two techniques have shown that the amorphous films transform to crystalline $\gamma\text{-Al}_2\text{O}_3$ after tempering above a critical temperature. XPS and UPS indicate that the films are stoichiometric and continuous down to the monolayer range. IRAS experiments of Al_2O_3 films on Au with thicknesses ranging between 3 and 200 Å show a striking thickness dependence of the vibrational frequency of the Al-O longitudinal mode. A similar thickness dependence is found for Al_2O_3 films on Al. This observation can be explained by the use of a simple model which is based on the fact that the restoring forces at the surface are smaller than in the bulk. The transition from amorphous Al_2O_3 to crystalline $\gamma\text{-Al}_2\text{O}_3$ is also reflected in the IRAS experiments of Al_2O_3 on Si and Al.

I. INTRODUCTION

Thin films on metals, such as oxide layers, sputtered dielectric films, or adsorbates, represent interesting systems in surface and interface physics as well as for applications.¹⁻⁷ Of basic interest is the question of how the physical properties change as a function of film thickness. Sufficiently thick films will exhibit bulk properties, but for very thin films in the region of a monolayer, properties characteristic of two-dimensional systems are expected. It is this transition from a three-dimensional (3D) to a two-dimensional (2D) system which is studied in this paper. The systems we are investigating are thin films of Al_2O_3 on gold, aluminum, and silicon, and the properties we are mainly interested in are the vibrational excitations in such films as studied by infrared reflection absorption spectroscopy (IRAS).⁸ The 3D-2D transition manifests itself in a very striking thickness dependence of the longitudinal optical (LO) vibrations associated with the stretching of the Al-O bonds.

Another interesting aspect lies in the fact that natural oxide layers of Al_2O_3 on Al are amorphous but transform to crystalline $\gamma\text{-Al}_2\text{O}_3$ after tempering.^{9,10} We have found that sputtered Al_2O_3 films on Au and Si are also amorphous, and that in the latter case a transition to crystalline $\gamma\text{-Al}_2\text{O}_3$ occurs after tempering above 750°C. The morphology of oxide films on metals is of basic importance for corrosion resistance.¹¹

The paper is organized as follows: Sec. II is devoted to a careful characterization of the Al_2O_3 films by means of transmission electron microscopy (TEM), low-angle x-ray spectroscopy, and x-ray and ultraviolet photoelectron spectroscopy (XPS and UPS). The latter two techniques indicate that sputtered Al_2O_3 films are stoichiometric and homogeneous down to thicknesses in the monolayer range (3–5 Å). In Sec. III the IRAS experiments of the systems $\text{Al}_2\text{O}_3/\text{Si}$, $\text{Al}_2\text{O}_3/\text{Au}$, and $\text{Al}_2\text{O}_3/\text{Al}$ are presented. In Sec. IV we give a discussion of the experimental results,

in particular of the thickness dependence of the LO frequency.

II. PREPARATION AND CHARACTERIZATION OF THE Al_2O_3 FILMS

Al_2O_3 films on Au and Si have been prepared by sputtering by using a Balzers Sputtrion 2 machine. The temperature of the substrate never exceeded 200°C during the sputtering process. The thicknesses of the films have been measured with a crystal quartz monitor. The accuracy in thickness is about ± 1 Å for a 10-Å-thick film. For low-angle x-ray scattering experiments and infrared transmission experiments of Al_2O_3 on silicon, an Al_2O_3 film with a thickness of 5100 Å has been sputtered on a polished surface of a Si(111) wafer (85–115 Ω cm) of 2 in. diameter and 0.25 mm thickness. For IRAS experiments of Al_2O_3 on Au, a thin gold film (500–1000 Å) was sputtered on glass plates. For IRAS measurements of Al_2O_3 on Al, bulk plates of Al have been used. Highly reflecting surfaces have been prepared by abrading with different grades of SiC paper, polishing with 3- μm diamond paste and with 0.05- μm MgO powder. The thickness of the natural oxide layer on Al is about 15–20 Å; this thickness has been determined indirectly by comparing the IRAS absorption of these plates with the absorption from Al_2O_3 films with known thicknesses sputtered on Au (Fig. 6). Thicker amorphous Al_2O_3 films on Al have been obtained by tempering in air up to 500°C, while crystalline $\gamma\text{-Al}_2\text{O}_3$ films on Al are obtained after tempering in air at 600°C for 12 h. $\gamma\text{-Al}_2\text{O}_3$ films on Si have been prepared by tempering at 1000°C in vacuum.

Figure 1 shows the intensity ratio of the Al 2s and O 1s XPS lines (inset in Fig. 1) for different thicknesses of the Al_2O_3 films on Au. This ratio is independent of thickness d for $3 < d < 200$ Å and the same as for bulk Al_2O_3 , indicating that the composition of the sputtered films is very close to stoichiometric Al_2O_3 . This implies that the sur-

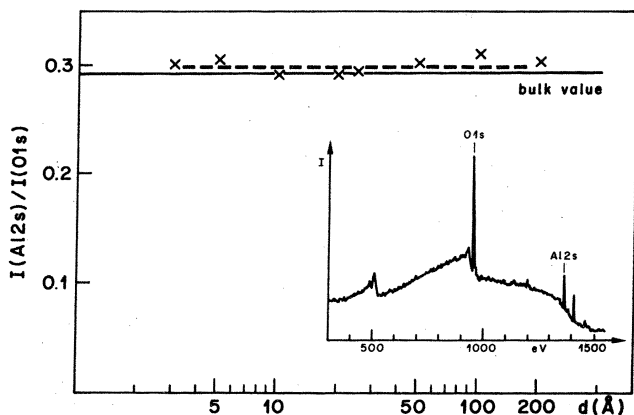


FIG. 1. Intensity ratio of the Al 2s and O 1s XPS lines (shown in the inset) for different thicknesses of Al_2O_3 films on Au. The corresponding bulk value has been determined to be 0.29.

face cannot be considered as an ideal termination of the bulk. The requirement of stoichiometry implies important rearrangements of the local structure.

The homogeneity in film thickness of the Al_2O_3 on Au has been investigated by XPS and UPS. The intensity of the Au 4f XPS line of the underlying gold substrate follows closely the relation $I(d) = I_0 \exp(-d/\lambda)$ with $\lambda = 19 \text{ \AA}$ in the thickness range from 100 to 5 \AA , which is compatible with films of homogeneous thicknesses. UPS spectra of pure Au, and of Au covered with 5 and 10 \AA of Al_2O_3 , have been studied with He II excitation. For the sample with 5 \AA of Al_2O_3 the 5d line of Au appears only as a weak shoulder on the valence-band structure of Al_2O_3 , and for the sample with 10 \AA of Al_2O_3 the Au signal disappears completely. Since the mean free path of UPS is only about 5 \AA , these results strongly indicate that the Al_2O_3 films are homogeneous down to thicknesses of about 5 \AA .

We have studied the morphology of sputtered Al_2O_3 films on Au; examination in the TEM showed no evidence of crystallinity for a 5000- \AA -thick film, even after sputtering off the gold substrate. This shows that the sputtered Al_2O_3 films on Au are amorphous. The same is true for Al_2O_3 films sputtered on Si(111) surfaces. Figure 2(a) shows the scattered x-ray intensity of a low-angle x-ray experiment, with an incident angle of 2° , performed with a 5100- \AA -thick Al_2O_3 film tempered at 500°C . The absence of the Bragg lines shows that the Al_2O_3 film is amorphous. After tempering at 1000°C , discrete Bragg lines appear [Fig. 2(b)] which can be identified with the lines of $\gamma\text{-Al}_2\text{O}_3$ [Fig. 2(c)].¹²

III. INFRARED EXPERIMENTS

All experiments have been carried out at room temperature with the use of a Perkin-Elmer 683 Infrared Spectrophotometer interfaced with a Perkin-Elmer Data Station. KRS5 polarizers were used in both the transmission and IRAS experiments. The transmission experiments of Al_2O_3 films on Si at normal and oblique incidence (Fig. 3) have been performed with a Si(111) wafer; an identical

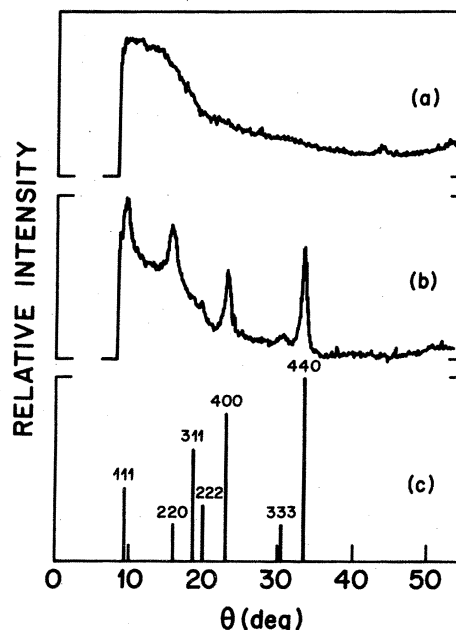


FIG. 2. Low-angle x-ray scattering of (a) Al_2O_3 after tempering of 10 h at 500°C , the absence of the Bragg lines shows that the Al_2O_3 layer is amorphous. (b) Crystalline $\gamma\text{-Al}_2\text{O}_3$, obtained after tempering of 1 h at 1000°C , and (c) x-ray lines of $\gamma\text{-Al}_2\text{O}_3$ from literature (Ref. 12).

wafer has been used as a reference. The IRAS experiments have been carried out using a modified multiple internal reflectance accessory. The angle of incidence was 60° and the light was 13 times reflected between the two parallel sample plates ($1 \times 13 \times 48 \text{ mm}$ and $1 \times 13 \times 57 \text{ mm}$, respectively).

The air gap between the sample plates was 1.5 mm. As a reference two gold mirrors in place of the sample plates have been mounted. From the sample and reference spectra, the absorption has been calculated using the CDS Data Station 68X.

A. The system $\text{Al}_2\text{O}_3/\text{Si}$

It is instructive to discuss first the transmission spectra of sputtered Al_2O_3 films on Si(111) as shown in Fig. 3. At normal incidence ($\alpha = 0^\circ$) only transverse optical (TO) modes with ionic displacements parallel to the film can be excited. The disorder in the amorphous film leads to a large number of oscillators in which the Al-O stretching modes are involved. Each of these modes has a certain nonvanishing dipole moment parallel to the film which can couple with the electric field of the light, and the collection of these modes, which is characterized by a distribution of oscillator strengths, causes a strong and broad infrared absorption; this constitutes the TO spectrum, which is centered near 690 cm^{-1} . This assignment is also supported by comparison with the results of an analysis of the phonon frequencies in corundum.^{13,14} The LO absorption associated with the strong TO absorption is observed in oblique incidence ($\alpha = 75^\circ$) at 950 cm^{-1} . At this angle there is a large component of the electric vector \vec{E} of the light perpendicular to the film which couples with the LO

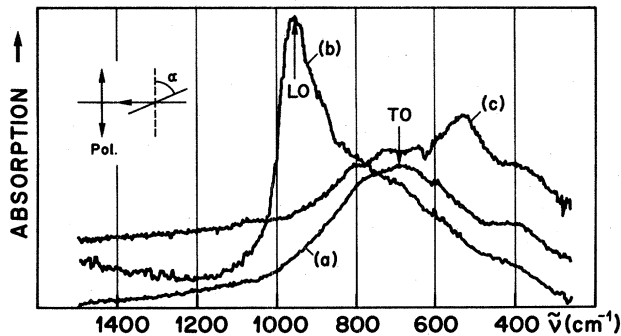


FIG. 3. Infrared transmission spectra of a 5100-Å-thick Al_2O_3 film on a Si(111) wafer. (a) Spectrum of an untempered, amorphous Al_2O_3 film at near-normal incidence ($\alpha=0^\circ$), showing the TO absorption. (b) Spectrum of the untempered, amorphous Al_2O_3 film at oblique incidence ($\alpha=75^\circ$), showing mainly the LO absorption. (c) Spectrum of the sample after tempering at 1000°C in vacuum, observed at normal incidence ($\alpha=0$), showing the TO spectrum of $\gamma\text{-Al}_2\text{O}_3$.

modes. The broad shoulder at the low-frequency side of the LO absorption is mainly due to the residual TO absorption caused by the small component of \vec{E} parallel to the film. The TO spectrum of the sample observed after tempering at 1000°C in vacuum shows additional structures which are associated with crystalline $\gamma\text{-Al}_2\text{O}_3$.

B. The system $\text{Al}_2\text{O}_3/\text{Au}$

Figure 4 shows the IRAS spectra of Al_2O_3 films sputtered on Au with film thicknesses ranging from 5 to 50 Å. In the IRAS configuration (inset of Fig. 4) only LO modes but no TO modes can be excited for sufficiently thin films. The LO modes are excited with p -polarized light, that is, by the component of \vec{E}_p perpendicular to the film. The components of \vec{E}_p parallel to the film as well as \vec{E}_s , the field for s -polarized light, are zero, because no electric field can exist parallel and adjacent to the metal surface¹⁵ (inset of Fig. 4). The absorption shown in Fig. 4 is therefore due to the LO mode; it appears at the same frequency as the LO mode of Al_2O_3 on Si (Fig. 3).

Figure 4 shows that the absorption peaks shift consider-

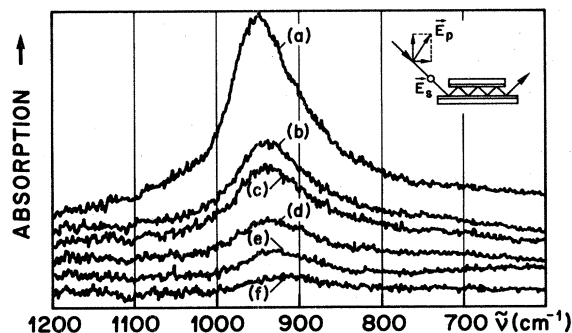


FIG. 4. IRAS spectra of Al_2O_3 films of various thicknesses d sputtered on Au. (a) $d=50$ Å, (b) $d=25$ Å, (c) $d=20$ Å, (d) $d=15$ Å, (e) $d=10$ Å, (f) $d=5$ Å. Note the decrease in the LO frequency with decreasing thickness.

ably to smaller frequencies with decreasing film thickness. This is seen more clearly in Fig. 5, in which the absorption peak of a 100-Å-thick film is compared with the (normalized and smoothed) absorption peak of a 5-Å-thick film: The frequency shifts from 950 to 910 cm^{-1} . On the other hand, the linewidths of the absorption peaks are constant and about 110 cm^{-1} in the whole thickness range between 200 and 5 Å. This large linewidth is due to the amorphous nature of the system which leads to a distribution in the frequencies and oscillator strengths as mentioned above. Figure 6 shows the thickness dependence of both the amplitude of the absorption peak as well as of the peak frequency in the range from 3 to 200 Å. The absorption is linear in film thickness in the whole thickness range. The peak frequency shows a pronounced thickness dependence: The frequency of a 2.5-Å-thick film, corresponding to about one monolayer of Al_2O_3 , is 905 ± 6 cm^{-1} ; with increasing thickness the frequency increases rapidly and saturates at about 100 Å to a value of 950 ± 2 cm^{-1} . The saturation frequency is identical with the bulk frequency observed for the LO mode of the thick Al_2O_3 film on Si (Fig. 3). The total relative frequency change is about 5%.

C. The system $\text{Al}_2\text{O}_3/\text{Al}$

Figure 7 shows the IRAS spectra of natural oxide films on bulk Al reflectors. The film thickness has been increased by tempering the same sample at different temperatures for 12 h. Additional measurements (not shown in Fig. 7) indicate that the oxidation kinetics are slow for temperatures below about 400°C and then increases rapidly up to 600°C, the highest temperature measured. Figure 7 shows that with increasing temperature both the absorption and the peak frequency increase. The film thicknesses have been determined by comparing the absorption with that of Al_2O_3 films on Au with known thicknesses (Fig. 6). A drastic change in the spectrum occurs at the phase transition from amorphous to crystalline $\gamma\text{-Al}_2\text{O}_3$, which takes place between 500 and 600°C. Above the phase transition we observe a very strong, broad and asymmetric absorption band with an additional shoulder near 800 cm^{-1} .

Figure 8 shows the thickness dependence of the LO frequency of natural Al_2O_3 films on Al. Our measurements

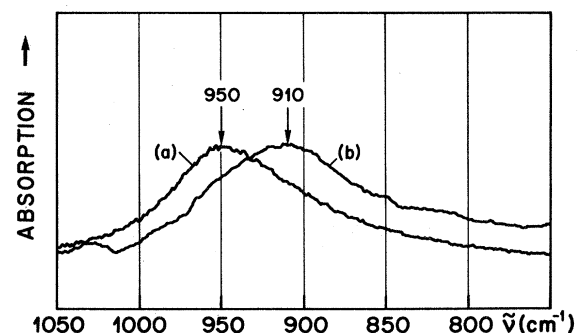


FIG. 5. IRAS absorption of two Al_2O_3 films on Au. (a) $d=100$ Å, (b) $d=5$ Å, scale expansion 20 \times , spectrum smoothed.

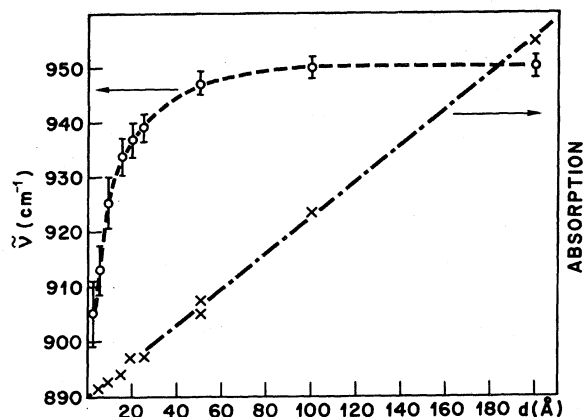


FIG. 6. Thickness dependence of the IRAS absorption of Al_2O_3 films on Au (\times) and of the peak frequency of the LO mode (\circ); (---), model calculation.

cover the experimental points in the thickness range between 106 and 16 Å; the latter value corresponds to the thickness of the natural oxide layer of an untempered sample. Experiments at smaller thicknesses would require *in situ* oxidation. The figure contains two experimental points at 888 and 848 cm^{-1} taken from Erskine and Strong.¹⁶ These authors studied the initial stage of oxidation of Al(111) by means of high-resolution electron energy-loss spectroscopy. The lower-frequency peak at 848 cm^{-1} is attributed to an Al—O stretching mode perpendicular to the surface involving oxygen at the threefold hollow site below the surface (subsurface oxygen), while the point at 888 cm^{-1} corresponds to the Al—O stretching mode of an Al_2O_3 layer with an estimated thickness of 3 Å.^{17,18} It is this latter point which can be directly compared with our experimental results, because it represents the vibrational frequency of approximately one monolayer of Al_2O_3 ; note that its frequency is fairly close to the “monolayer frequency” of 905 cm^{-1} of Al_2O_3 on Au (Fig. 6). Apart from slight systematic deviations which are probably due to slightly different densities of the films,¹⁹ the qualitative behavior of $\bar{\nu}(d)$ is the same for the two systems $\text{Al}_2\text{O}_3/\text{Au}$ and $\text{Al}_2\text{O}_3/\text{Al}$.

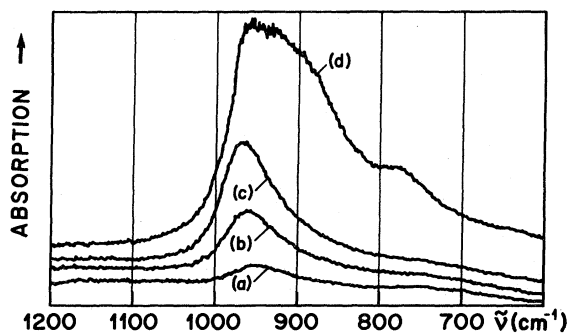


FIG. 7. IRAS absorption of natural Al_2O_3 films on Al. (a) Untempered sample, (b) after tempering in air for 12 h at 400°C, (c) at 500°C, (d) at 600°C. The phase transition from amorphous Al_2O_3 to crystalline $\gamma\text{-Al}_2\text{O}_3$ occurs between 500 and 600°C.

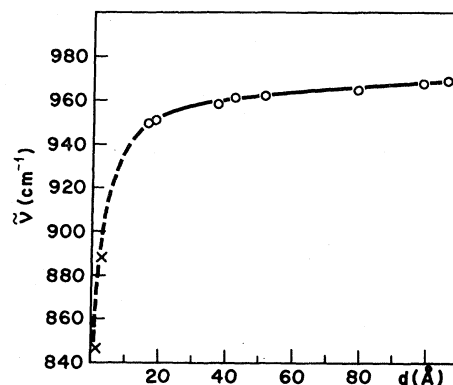


FIG. 8. Thickness dependence of the LO vibrational frequency $\bar{\nu}_{\text{LO}}$ of natural Al_2O_3 films on Al. \circ , our measurements; \times , from electron energy-loss spectroscopy (Ref. 16). The point at 848 cm^{-1} corresponds to “subsurface oxygen,” while the point at 888 cm^{-1} corresponds to an Al_2O_3 layer of about 3 Å thickness (Refs. 17 and 18).

IV. DISCUSSION

In this section we discuss the thickness dependence of the LO vibrational frequency as shown in Figs. 6 and 8. As discussed in Sec. II the effect of the surface together with the requirement of stoichiometry must give rise to complicated rearrangements of the local geometry. The most simple model is based on the fact that due to the missing bonds at or close to the surface the mean restoring force $\langle F \rangle$ acting on an ion near the surface is lower than in the interior of the film. We can also think in terms of a mean coordination number of an ion which increases slightly in going from the surface into the bulk; this increase will be associated with a corresponding increase of $\langle F \rangle$. To simplify the calculations we have adopted an Einstein model by assuming that the Al^{3+} ions are moving independently in the rigid cages formed by the O^{2-} ions. In the interior of the film $\langle F \rangle$ is equal to the bulk value F_b but decreases to slightly lower values at the surfaces. The simplest description of this effect would be the use of a smaller restoring force F_s just at the surface layer. This leads to a faster saturation of the average frequency than observed (Fig. 6). One is led therefore to extend the variation of the restoring force to more than just the surface layer. Figure 9 illustrates this situation schematically by introducing appropriate force constants g_s , $g_1 = g_s + \epsilon$, $g_2 = g_s + 2\epsilon$, $g_3 = g_s + 3\epsilon$, where g_s is a surface force constant and ϵ is a small increment. Note that our g 's represent a measure for the product of the average number of bonds and the bond strength. For a film containing n layers the mean eigenvalue $\langle \lambda_n \rangle$ is then proportional to

$$\langle \phi_n \rangle = \frac{1}{n} \sum_{l=1}^n K_{nl},$$

where $\langle \phi_n \rangle$ is the mean force constant and K_{nl} is the force constant of layer l in the n -layer system. Thus $K_{11} = 2g_s$, $K_{21} = K_{22} = g_s + g_1$, $K_{31} = K_{33} = g_s + g_1$, $K_{32} = 2g_2$, etc. (Fig. 9). For very thin films (some monolayers) the surface effects will be important, resulting in a comparatively low frequency. With increasing thickness

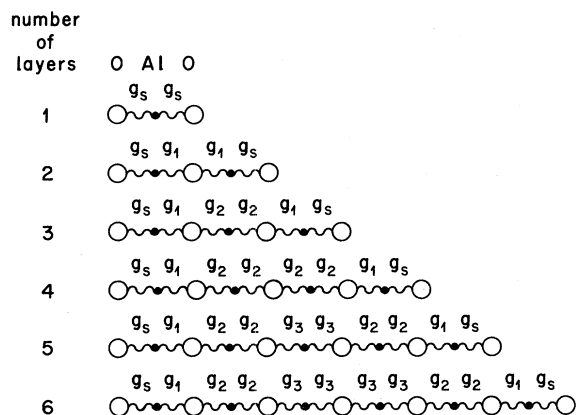


FIG. 9. Schematic representation of Al_2O_3 films containing 1–6 monolayers. In reality a single amorphous monolayer does not have the composition AlO_2 but rather Al_2O_3 . $g_s, g_1 = g_s + \epsilon, g_2 = g_s + 2\epsilon, g_3 = g_s + 3\epsilon$ are the force constants of the Einstein model (see text).

the surface effects become less important leading to a saturation of the frequency at the bulk value. Given the bulk force constant g_b the model contains two parameters, namely the surface force constant g_s and the distance from the surface at which the bulk value is reached. In more refined models the restoring force profile will not be completely symmetric because one surface is in contact with Au (or Al), the other with air. Experiments using a 30-Å-thick gold overlayer on top of the Al_2O_3 film indicate a very small increase of the vibrational frequency which is probably due to hard-core interactions between oxygen ions and gold atoms. Neglecting this asymmetry we have calculated the normalized $\bar{\nu}(d)$ curve using the following parameters: $g_s = 0.91g_b$, a relaxation length of two monolayers and therefore $\epsilon = 0.03$; note that in this case $g_b = g_3$ (Fig. 9). The results for $\text{Al}_2\text{O}_3/\text{Au}$ are shown in Fig. 6. A very good agreement with experiments is achieved.

IRAS studies of natural Al_2O_3 layers on Al have been performed before.^{20–23} Mertens has studied the oxidation of aluminum single crystals.²⁰ In qualitative agreement with our results (Fig. 8) he finds an increase of the LO frequency with increasing film thickness, but no explanation is given. As far as the authors are aware this study represents the first investigation of the thickness dependence of vibrational frequencies in the range between several hundred angstroms down to monolayer thicknesses. This thickness range is of great importance because it allows the investigation of the change in physical properties associated with the 3D-2D transition.

At this point it should be mentioned that considerable experimental and theoretical studies have been performed on adsorbates in the submonolayer region; examples are CO on Pt and halides adsorbed on silver.^{24–27} It is generally found that the vibrational frequencies of the adsor-

bate also decrease with decreasing fractional coverage Θ ($0 \leq \Theta \leq 1$, $\Theta = 1$ corresponds to one monolayer). This effect has been explained in terms of long-range dipole-dipole coupling including the image dipoles in the metallic substrate.²⁴ Long-range dipole-dipole coupling is certainly an important mechanism for molecular adsorbates with fractional coverages. Our system is, however, different from submonolayer adsorbates not only because of the larger thickness, but also because Al_2O_3 is not a molecular compound. As a consequence, there are necessarily missing bonds at the surface, the effect of which on the vibrational frequencies can be described by our simple model. Dipole-dipole interactions will also contribute to the observed frequency shift in Al_2O_3 , but the good description obtained with the short-range force constants suggests that the dipole-dipole interaction is of minor importance. If long-range dipole-dipole coupling would be the dominating mechanism, we would also expect a considerably slower saturation of the mean frequency.

Vibrational properties of thin films including ionic slabs have been studied extensively. Two methods have been used. The first is the continuum approximation first used by Fuchs and Kliewer²⁷ for a slab with two flat surfaces. The second method involves lattice-dynamical calculations for a slab-shaped crystal.^{28–34} The continuum approximation is valid only at large wavelengths in a thick slab and cannot be applied to our systems. Lattice-dynamical calculations have only been performed for well-ordered structures, such as NaCl, and GaAs.³⁴ In the latter case the variation of the LO frequency with film thickness has been calculated and a similar qualitative behavior has been found as in our experiments. On the other hand, the two systems cannot be compared directly because our system is amorphous and GaAs is ordered. This is probably the reason why in our case the saturation of the frequency is slower than for GaAs.

In conclusion our studies have shown that the Al_2O_3 films on Au are stoichiometric and homogeneous down to the monolayer range. The IRAS absorption varies linearly with thickness and the vibrational frequency of the Al–O longitudinal mode shows a striking thickness dependence, a similar thickness dependence is found for Al_2O_3 films on Al. This observation can be explained by using a simple model which is based on the fact that the restoring forces at the surface are smaller than in the bulk. Finally, the transition from amorphous Al_2O_3 to crystalline γ - Al_2O_3 is evidenced in low-angle x-ray scattering as well as in IRAS experiments of Al_2O_3 on silicon and on aluminum.

ACKNOWLEDGMENTS

The authors are indebted to Professor A. A. Maradudin and Professor T. M. Rice, and Dr. S. Strässler for interesting discussions, and to Dr. R. Hutchings for the TEM experiments. We also would like to thank Mr. R. Weder, W. Foditsch, and J. Voboril for excellent technical assistance.

- ¹*Interactions on Metal Surfaces*, Vol. 4 of *Topics in Applied Physics*, edited by R. Gomer (Springer, Berlin, 1975).
- ²*Chemistry and Physics of Solid Surfaces IV*, Vol. 20 of *Springer Series in Chemical Physics*, edited by R. Vanselow and R. Howe (Springer, Berlin, 1982).
- ³K. L. Chopra, *Thin Film Phenomena* (McGraw-Hill, New York, 1969).
- ⁴*The Use of Thin Films in Physical Investigations*, edited by J. C. Anderson (Academic, London, 1966).
- ⁵*Proceedings of the Symposium on Thin Film Interfaces and Interactions*, edited by J. E. E. Baglin and J. M. Poate (Electrochemical Society, Princeton, New Jersey, 1980), Vol. 80-2.
- ⁶*Thin Film Dielectrics*, edited by F. Vratny (Electrochemical Society, New York, 1969).
- ⁷*Physics in Thin Films*, edited by G. Hass and M. Francombe (Academic, New York, 1980), Vol. 11.
- ⁸H. G. Tompkins, in *Method of Surface Analysis*, edited by A. W. Czanderny (Elsevier, Amsterdam, 1975), Vol. 1, Chap. 10, p. 477.
- ⁹G. Haas, *Z. Anorg. Chem.* **254**, 96 (1947).
- ¹⁰K. Shinohara, T. Seo, and H. Kyogoku, *Z. Metallkd.* **73**, 774 (1982).
- ¹¹A. G. Revesz and J. Kruger, in *Passivity of Metals* (Proceedings of the Fourth International Symposium on Passivity), edited by R. P. Frankenthal and J. Kruger (Electrochemical Society, Princeton, New Jersey, 1978).
- ¹²*Powder Diffraction File, Inorganic Phases*, edited by W. F. McClune (International Centre for Powder Diffraction Studies, Swarthmore, 1981).
- ¹³K. Iishi, *Phys. Chem. Miner.* **3**, 1 (1978).
- ¹⁴A. S. Barker, Jr., *Phys. Rev.* **132**, 1474 (1963).
- ¹⁵D. W. Berreman, *Phys. Rev.* **130**, 2193 (1963).
- ¹⁶J. L. Erskine and R. L. Strong, *Phys. Rev. B* **25**, 5547 (1982).
- ¹⁷B. E. Hayden, W. Wyrobisch, W. Oppermann, S. Hachicha, P. Hofmann, and A. M. Bradshaw, *Surf. Sci.* **109**, 207 (1981).
- ¹⁸M. Bujor, L. A. Larson, and H. Poppa, *J. Vac. Sci. Technol.* **20**, 392 (1982).
- ¹⁹This is supported by the fact that the observed frequencies of the system $\text{Al}_2\text{O}_3/\text{Al}$ prepared by *sputtering* are identical with the frequencies of the system $\text{Al}_2\text{O}_3/\text{Au}$ in the thickness range between 15 and 200 Å. Below 15 Å, oxidation of the underlying Al substrate sets in, which leads to deviations in $\bar{\nu}(d)$.
- ²⁰F. P. Mertens, *Surf. Sci.* **71**, 161 (1978).
- ²¹A. J. Maeland, R. Rittenhouse, W. Lahar, and P. V. Romano, *Thin Solid Films* **21**, 67 (1974).
- ²²S. Thibault and C. Duchemin, *Corrosion (USA)* **35**, 532 (1979).
- ²³J. Chatelet, H. H. Claassen, D. M. Gruen, I. Sheft, and R. B. Wright, *Appl. Spectrosc.* **29**, 185 (1975).
- ²⁴H. Nichols and R. M. Hexter, *J. Chem. Phys.* **73**, 965 (1980).
- ²⁵H. Nichols and R. M. Hexter, *J. Chem. Phys.* **76**, 5595 (1982).
- ²⁶G. D. Mahan and A. A. Lucas, *J. Chem. Phys.* **68**, 1344 (1978).
- ²⁷R. Fuchs and K. L. Kliewer, *Phys. Rev.* **140**, A2076 (1965).
- ²⁸A. A. Lucas, *J. Chem. Phys.* **48**, 3156 (1968).
- ²⁹S. Y. Tong and A. A. Maradudin, *Phys. Rev.* **181**, 1318 (1969).
- ³⁰W. E. Jones and R. Fuchs, *Phys. Rev. B* **4**, 3581 (1971).
- ³¹T. S. Chen, G. P. Alldredge, and F. W. de Wette, *Phys. Rev. Lett.* **26**, 1543 (1971).
- ³²G. Kanellis, J. F. Morhange, and M. Balkanski, *Phys. Rev.* **28**, 3390 (1983).
- ³³G. Kanellis, J. F. Morhange, and M. Balkanski, *Phys. Rev.* **28**, 3398 (1983).
- ³⁴G. Kanellis, J. F. Morhange, and M. Balkanski, *Phys. Rev.* **28**, 3406 (1983).